

# Analytical Study of 2D Integrated Microcantilever Pressure Sensing of Fluid for Healthcare Application

Ankur Saxena<sup>1</sup>, Mahesh Kumar<sup>2</sup> and Kulwant Singh<sup>1\*</sup>

<sup>1</sup>FlexMEMS Research Center, Department of Electronics & Communication Engineering, Manipal University Jaipur, Jaipur-303007, Rajasthan, India.

<sup>2</sup>Department of Computer Science and Engineering, Graphic Era Deemed to be University Dehradun, Dehradun 248001, Uttarakhand, India.

## Abstract

The proposed work focusses on the 2D design and modelling of integrated microcantilever in microchannel for the analysis of fluid pressure. In order to compute the microfluidic pressure in microchannel at various angles, fluid structure interaction is analyzed using the finite element method. With a fluid flow rate of 4.33 cm/s, a 2D integrated microcantilever can optimize both fluid pressure and microcantilever deflection. The novelty of the microfluidic pressure sensing mechanism allows pressure of fluid to be sensed in a microchannel without connecting any electrical method such as piezoresistor or piezoelectric approach. The objective of the research is to integrate a microcantilever into a microchannel to reduce setup complexity and procedure cost. Maximum deflection of the 2D T-microcantilever achieved 10.30 $\mu$ m at, pressure at the tip of T-microcantilever 10.89 Pa, fluid velocity 0.00309 m/sec, and Reynolds number is 1.22

**Keywords:** Microcantilever, Microfluidic, Pressure Sensing, Velocity, T-microcantilever, Cutoff position

## 1.0 Introduction

Application of microfluidics pressure sensing is extensively applicable in the field of biological<sup>1</sup>, chemical sensing<sup>2</sup>, cell separation/sorting<sup>3</sup>, and drugs delivery<sup>4</sup> has enormous potential. These type such of applications are extremely depending on flow rate of fluid flow across a microchannel. The controlling of fluid and measuring a pressure across a microchannel is a precise significant functionality in microfluidics field. Numerous pressure sensing mechanism have been reported in the literature by integration methodology of MEMS device for microfluidic application. As a result of fluid pressure being applied, an integrated microcantilever top surface was deflected and bending down was being measured<sup>5</sup>. The microcantilever's bending capabilities are a crucial component, and bending microcantilever requires elastic

material with strong tensile strength. Microcantilever deflection in a micrometer requires sophisticated optical or electrical equipment for deflection measuring<sup>6</sup>. However, the application of this optical fiber cantilever sensor in microfluidics is restricted. Similar to electrical sensors, biological cells' toxic nature limits their use and poses challenges for electrical sensors<sup>7</sup>. Silicon and SU-8 are frequently utilized to create microcantilever, but because of their strong elastic properties and toxic behaviour, they do not produce results that are suitable for living cells or applications in medical equipment<sup>8,10</sup>. For the detection and elimination of a toxic problem, the low elastic modulus material PDMS is a suitable alternative<sup>11,12</sup>. Different sensing mechanisms can be utilized to measure the fluid pressure in microchannel, such as deforming PDMS, forming a PSP sensing layer on a microcantilever, and measuring the pressure using optical microscopy. Another option is to design a galinstain bridge circuit and measure the fluid pressure using the piezoresistive

\*Corresponding Author

or piezoelectric method<sup>13,14</sup>. Different types of algorithms are used to identify the deflection of a vertical PDMS microcantilever or beam in order to sense or measure the force of cells. Higher sensitivity and a linear response device were needed for the flow detection approach in order to achieve this; low aspect ratio PDMS material has low stiffness<sup>15-17</sup>. Experimental microchannel designed by SU8 material on using wafer of silicon, by the process of photolithography's and soft baking<sup>18</sup>.

In this paper, design and simulation of various types of integrated microcantilever across a microchannel, paper demonstrate a 2D-microfluidic pressure sensing mechanism with numerous types of investigation of integrated microcantilever across a microchannel<sup>19</sup>. Two-dimensional structure designed on COMSOL tool, fluid flow from inlet to outlet across a microchannel, dimension specification of microchannel length and width are respectively; 400 $\mu$ m and 200 $\mu$ m. Integration of two physics properties laminar fluid flow and solid mechanics with the device and characterized fluid characteristics. 2D-simulation analysis of microfluidic device is classified in three categories (i) analysis of microcantilever at distinct locations across a microchannel (ii) simulation various types of microcantilever T-microcantilever, rectangular microcantilever, Pi-microcantilever across a microchannel (iii) analyzing T-microcantilever at the distinct vertical cutoff point position. 2D simulation and analysis of fluid, measure tip deflection of microcantilever with respect to the time domain or time-dependent. The results of simulation at various aspect and found T-microcantilever provide maximum displacement of 10.38  $\mu$ m at time 0.215 sec, while pressure and fluid velocity value measured 10.89 Pa and 0.0302 m/sec. microcantilever provides substantial outcomes at a low laminar fluid velocity.

## 2.0 Geometry of Integrated Microcantilever

Fig.1 shows different position of rectangular microcantilever from the inlet, fluid flow inlet at very high pressure the as rectangular microcantilever which is placed near by the inlet

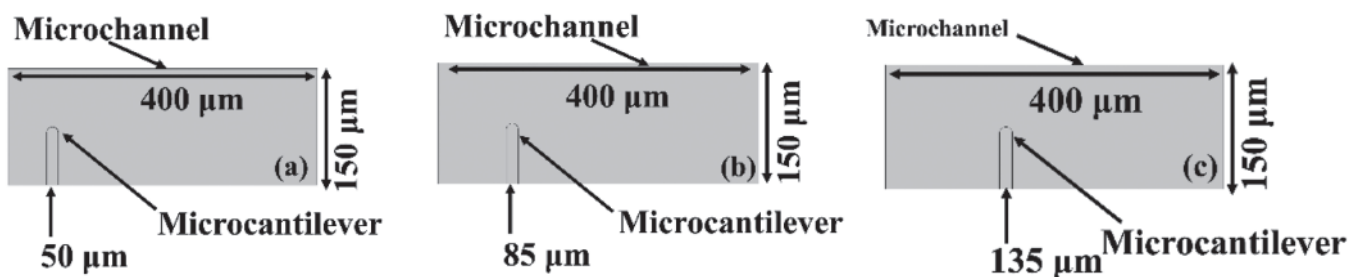


Figure 1: Microcantilever schematic structure with its position and dimensions (a)  $\mu$ cantilever fixed in microchannel at 50  $\mu$ m distance from inlet (b)  $\mu$ cantilever fixed in microchannel at 85  $\mu$ m distance from inlet (c)  $\mu$ cantilever fixed in microchannel at 135  $\mu$ m distance from inlet with dimensions

port give maximum deflection. The geometry of integrated of microcantilever across a microchannel is shown in Fig.1 Rectangular microcantilever, Pi-microcantilever, and T-microcantilever placed at 50  $\mu$ m, 85  $\mu$ m and 135  $\mu$ m. 2D geometry design in COMSOL multiphysics focusing on length and height of microcantilever. The two physics are combined in FSI (Fluid Structure Interaction) laminar fluid flow and solid mechanics. Microcantilever deformed due to applied pressure on its body when the fluid flow across a microchannel. Microcantilever tip change its position from original position to apparent position due to applied pressure of fluid. Tip deflection of microcantilever gives a minor strain with corresponding mean velocity of fluid<sup>20</sup>.

Proposed 2D integrated microcantilever microfluidic device is shown in the Fig.2 with microchannel. Fluid flow across microchannel with parabolic profile and connected with microcantilever. The simulation is done COMSOL tool with time dependent study, time range defined (0, 0.005, 0.75) and (1, 0.25, 4) fluid velocity, pressure and stress examined with respect to time<sup>21</sup>. The Fig.3 shows T-microcantilever numerous cutoff locations where fluid applied a pressure and cantilever get deflected, deflection of microcantilever is calculated by COMSOL tool. The materials used in designing of integrated microcantilever pressure sensor across microchannel for detection of pressure sensing mechanism. The PDMS material is preferred on basis of two factors, material should be not more rigid and young modulus should not be too high. Properties of micro cantilever are Young's modulus 2e5 Pa, poisson's ratio 0.33, and density 7850 Kg/m<sup>3</sup>. Fluid properties define with density and dynamic viscosity in COMSOL Tool. Fluid flows across microchannel contact with microcantilever, if water property density or dynamic viscosity is precisely high, fluid flow became precisely slow and T-microcantilever is not able to deflect due to its low velocity of a water. So here water dynamic viscosity and density are respectively defining 10<sup>-3</sup> Pa.s and 1000 kg/m<sup>3</sup>

## 3.0 Methodology

ALE (Arbitrary Lagrangian Eulerian) technique is applied to combine fluid flow expressed consuming an Eulerian

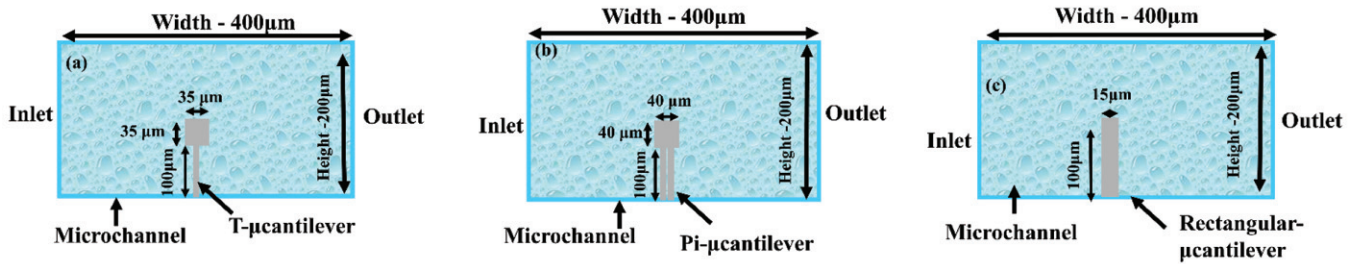


Figure 2: Microcantilever schematic structure with specified dimensions (a) T  $\mu$ cantilever is placed in microchannel at 2000  $\mu$ m distance from inlet and dimensions are shown (b) Pi  $\mu$ cantilever is placed in microchannel at 2000  $\mu$ m distance from inlet with dimensions (c) Rectangular microcantilever is placed in microchannel at 2000  $\mu$ m distance from inlet with dimensions

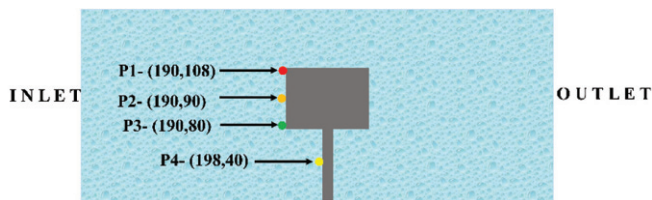


Figure 3: T-Microcantilever schematic structure with its cut off point position

description and spatial frame with solid mechanics expressed using a lagrangian method<sup>22</sup>. Laminar fluid flow across a microchannel; it is incompressible and steady flow liquid, and microcantilever situated across a microchannel, bottom end of microcantilever is fixed and connected with the bottom surface of microchannel<sup>23</sup>. The fluid flow 4.33 cm/sec velocity across a microchannel, parabolic velocity profile fluid interacts with a microcantilever, microcantilever tip surface got maximum pressure and effect of pressure moves its top surface from its original position to apparent position as show in Fig.4 at time from 1 sec to 4 sec with an break of 0.01 sec. Each structure gives some significant result of various shapes in terms of deflection, pressure, stress, at various simulation times.

Laminar fluid flow across a microchannel, with constant velocity fluid flow a microcantilever sense its velocity and microfluidic pressure. Laminar fluid flow governs equation for the processing of fluid flow across microchannel. Incompressible fluid flow across a microchannel with no slip condition of wall at temperature 293.15K. The Navier's Stokes equation in fluid mechanics is given such types:

$$\rho \frac{\partial u}{\partial t} + \rho(u \cdot \nabla)u = \nabla \cdot [-pI + K] + F \quad \dots (1)$$

The incompressible flow gives the continuity equation for the fluid flow across a microchannel with density  $\rho$ , velocity  $u$  and no source and sink written as;

$$\rho \frac{\partial u}{\partial t} + \nabla(\rho \cdot u) = 0 \quad \dots (2)$$

Then introduce the differential operator

$$\frac{D}{Dt} = \frac{\partial}{\partial t} + u \cdot \nabla \quad \dots (3)$$

The continuity equation can be represented in this form is shown in equation 4. The incompressible fluid flow density is constant, so continuity equation differential part becomes zero as shown in equation 5.

$$\frac{D\rho}{Dt} = \frac{\partial \rho}{\partial t} + \rho \nabla \cdot u \quad \dots (4)$$

$$\rho \nabla \cdot u = 0 \quad \dots (5)$$

The laminar characteristics established parabolic profile along microchannel, transformation in amplitude with respect to time<sup>24</sup>. The velocity fixed amplitude given by equation:

$$u_{in} = \frac{U_{\infty} x^2}{\sqrt{(0.004 - t^2)^2 + (0.1t)^2}} \quad \dots (6)$$

Fluid flow have a relation with Reynold's number, its defined type of fluid. Reynold's number calculated on basis of dimension and material properties of fluid like dynamic viscosity and density. 2D microstructure where water as a fluid taken with fluid dynamic viscosity and density were respectively 0.001 Pa.s and 1000 kg/m<sup>3</sup>. Fluid velocity is directly proportional to Reynold's number, Reynold's number value high show turbulent flow of fluid while if Reynold number values lie <2000 then its show laminar fluid. The Reynold's number calculated as a given equation:

$$Re = \frac{\rho v D_h}{\mu} \quad \dots (7)$$

Laminar fluid flows the general relation for semi-circular channel is given by  $f = K/Re$  where  $f$  is fanning friction factor and  $K$  is numerical coefficient that depends on the shape of microchannel

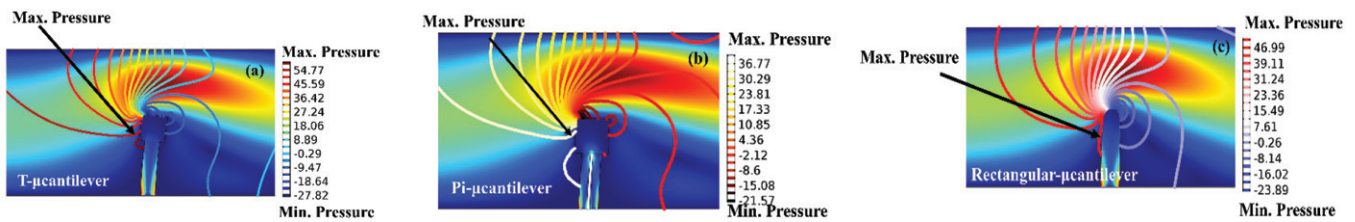


Figure 4: 2D-Microcantilever simulated design analysis (a) T  $\mu$ -cantilever deflected when fluid flow left hand side to right side and max deflection achieved (b) Pi  $\mu$ -cantilever deflected when fluid flow left hand side to right hand side (c) T  $\mu$ -cantilever deflected when fluid flow left hand side to right side and max deflection achieved

## 4.0 Result and Discussion

### 4.1 Analysis of fluid velocity across microchannel at distinct location of microcantilever

Microcantilever placed across microchannel; a fluid flow from inlet to outlet and its properties of fluid varies along the distance. Microcantilever placed at various positions across microchannel for analysis of pressure and velocity profile. Microcantilever placed at 50  $\mu\text{m}$ , 80  $\mu\text{m}$ , and 135  $\mu\text{m}$  from an inlet of a microchannel, fluid properties examined at time domain. The velocity maximum achieved at 50  $\mu\text{m}$ , now microcantilever change its position from 50 to 80 then 135 and found when distance increased then fluid velocity become lower and due to its deflection in microcantilever become less as shown in Fig.5. The velocity varies with respect to time gradually increasing until time 0.215 sec a fluid velocity maximum achieved when microcantilever closed to inlet position at 50  $\mu\text{m}$ . The velocity of microfluidic is very high when microcantilever at 50  $\mu\text{m}$  due to its deflection occurs in microcantilever, which was also high at 50  $\mu\text{m}$  in comparison with 80  $\mu\text{m}$  and 135  $\mu\text{m}$ .

### 4.2 Analysis of Pressure at distinct position of microcantilever across/in microchannel

Controlling the fluid flow rate across a microchannel, numerous possibilities are available but operating technique increased in price of device. Pressure controlling of fluid have features of reliable, extremely efficient and measure pressure at individually. Microcantilever placed at positions 50  $\mu\text{m}$ , 85  $\mu\text{m}$ , and 135  $\mu\text{m}$  measure pressure of microfluidic, maximum pressure at time 0.005 sec, 0.215 sec, and 4 sec. Fig.6 shows variation of pressure at different position of microcantilever and found distance of microcantilever increased from inlet position, pressure value also decreased. The maximum pressure 31.93 Pa achieved at 50  $\mu\text{m}$  while minimum pressure attained at 200  $\mu\text{m}$ .

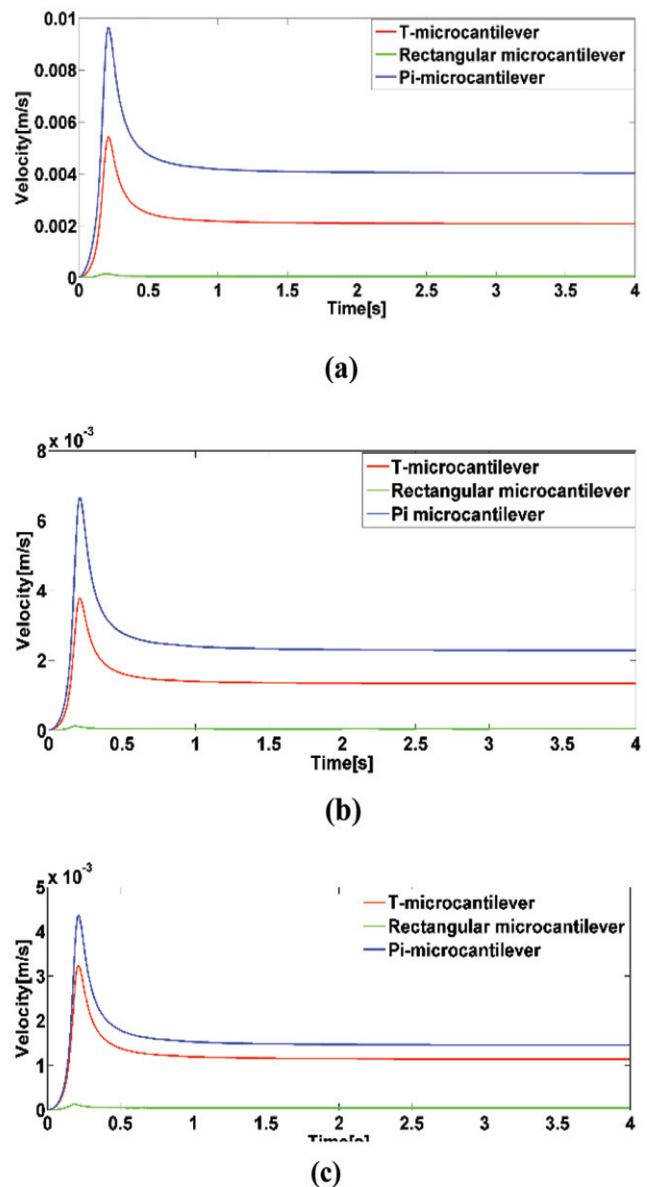
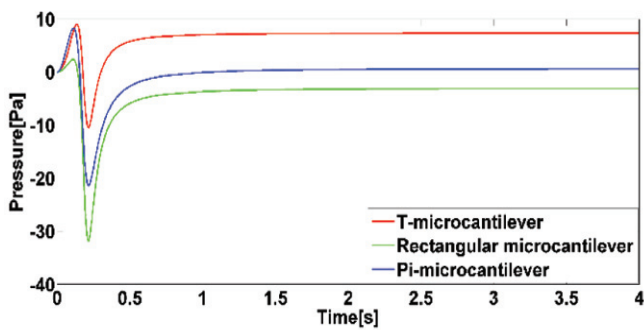
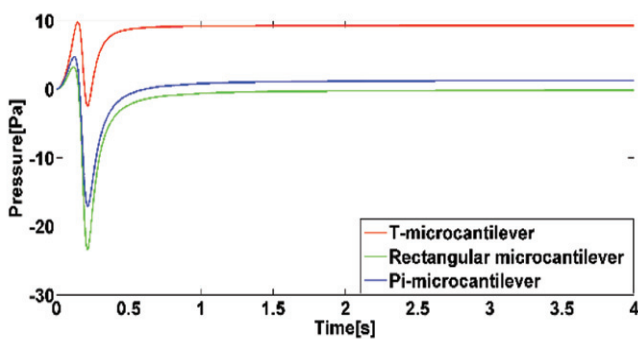


Figure 5: Velocity varies with time at various position of rectangular microcantilever (a) Velocity at 50 $\mu\text{m}$  (b) Velocity at 85 $\mu\text{m}$  (c) Velocity at 135 $\mu\text{m}$

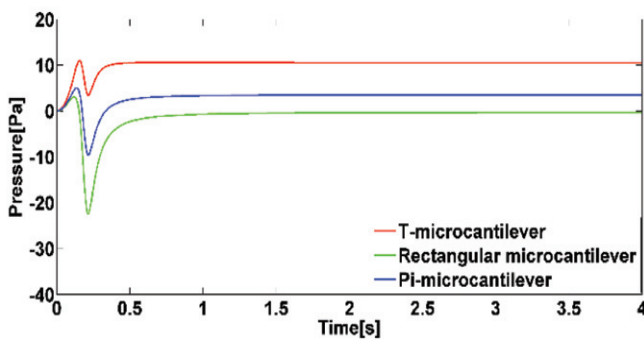




(a)



(b)



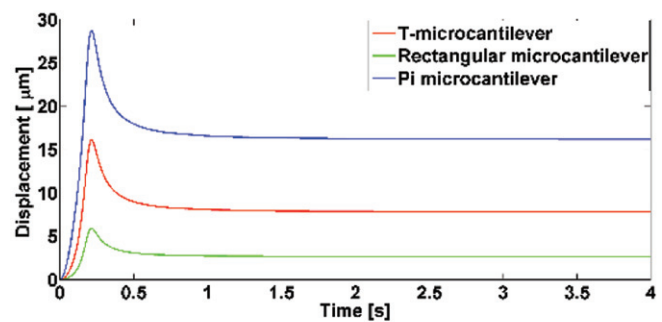
(c)

Figure 6: Pressure varies with time at various position of rectangular microcantilever (a) Pressure at 50µm (b) Pressure at 85µm (c) Pressure at 135µm

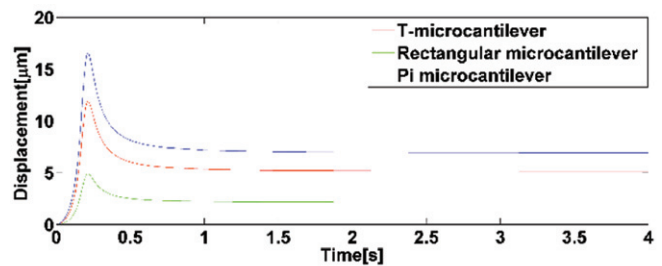
Fig.6 shows pressure of fluid in beginning; it is almost stable there no variation occurred but as velocity increased pressure of fluid also increased and it bended down microcantilever so pressure increased in negative y-axis direction as overshoot value achieved now pressure start to decreased due to this it achieved minimum value after pressure became in steady state condition.

### 4.3 Analysis of displacement at distinct position of microcantilever across/in microchannel

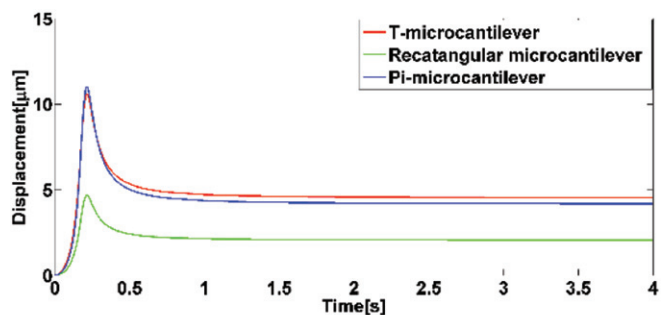
The fluid flow across microchannel a microcantilever placed at a distinct location, deflection occurred when pressure applied on surface of microcantilever. The COMSOL tool measure deflection, and found when microcantilever at 50 µm maximum deflection occurs 5.921 µm at time 0.215 sec. while minimum deflection achieved 2.060 µm at 200 µm. It shows displacement occurs with respect to time of rectangular microcantilever at numerous position. Fig.7



(a)



(b)



(c)

Figure 7: Displacement varies with time at various position of rectangular microcantilever (a) Displacement at 50 µm (b) Displacement at 85 µm (c) Displacement at 135 µm

shows graph between displacement and time, location of microcantilever is shown in graph overshoot value is attained at 50  $\mu\text{m}$  distance, while minimum value is attained at 200  $\mu\text{m}$ .

#### 4.4 Comparative analysis fluid velocity at centre of microchannel

Analysis of fluid velocity effect on microcantilever, as fluid interact with microcantilever its deflected from its original position to apparent position. Rectangular microcantilever gives minimum velocity when fluid interact with it and T-microcantilever gives maximum velocity at time 0.21 sec. The Fig.8 shows the graph between velocity and time for rectangular microcantilever, Pi-microcantilever and T-microcantilever. The analysis is focus on maximum displacement when achieved that time fluid velocity is rectangular is 0.00306 m/s, Pi-microcantilever 0.00311 m/s and T-microcantilever 0.0011 m/sec. The graph easily defines that in the beginning the fluid velocity continuously increased after some time its velocity decreased and finally its achieved saturated state with respect to time. The overshoot value achieved at 0.215 sec after that the fluid velocity becomes decreasing and achieved at minimum values at time 0.5 sec after that velocity became in a steady-state condition of its. Now overshoot values of T-microcantilever and Pi-microcantilever are almost the same so that both graphs overlapped to each other. The velocity of the fluid at T-microcantilever is maximum due to the hinged structure of it, a top surface of the microcantilever gives maximum deflection at 0.003071 m/sec.

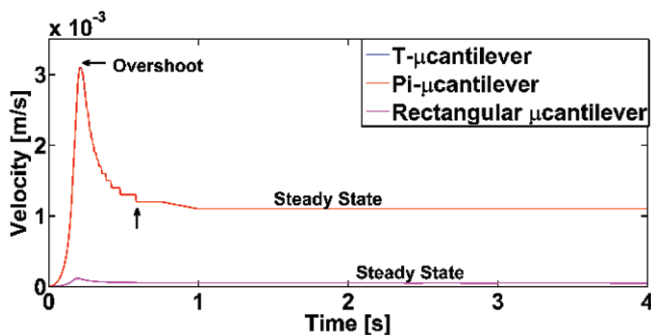


Figure 8 Velocity varies with time for T-microcantilever, Pi-microcantilever and rectangular microcantilever

#### 4.5 Comparative analysis fluid Pressure at centre of microchannel

Pressure sensing<sup>27</sup> is an imperative factor to measure in microchannel for laminar fluid flow, fluid-applied pressure on microcantilever to shift its position from original to apparent. The microcantilever describes pressure-sensing mechanism,

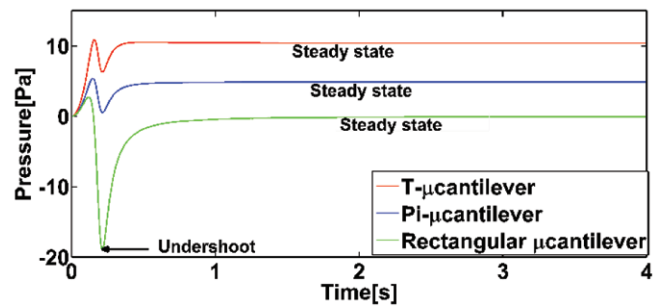


Figure 9: Pressure varies with time for T-microcantilever, Pi-microcantilever and rectangular microcantilever

pressure of fluid, which was flowing across a microchannel, measurement of deflection at various times<sup>28</sup>. Microcantilever studied and plot graph between pressure and time as shown in Fig.9. The overshoot value of pressure achieved by T-microcantilever 10.894 Pa at time 0.16 and minimum value 6.93 Pa at time 0.235sec. Similarly at same time Pi-microcantilever achieved 5.422 Pa at time 0.16 sec and rectangular microcantilever achieved 2.728 Pa at time 0.16 sec. if discussed the overshoot point of Pi-microcantilever and rectangular microcantilever are 5.4227 Pa at time 0.15 sec and 2.7286 Pa at time 0.12, while discussing minimum value point of rectangular microcantilever is 18.937 Pa at time 0.22 second. A microcantilever pressure increased with an increase in time as peak pressure achieved then pressure starts decreasing after some time it moves in a steady-state condition.

#### 4.6. Comparative Analysis Displacement Microcantilever at Centre of Microchannel

Fig.10 shows comparative analysis of microcantilever, maximum displacement achieved by T-microcantilever and minimum displacement achieved by rectangular microcantilever. The displacement value is high representing bending of the large movement of microcantilever due to high pressure of a fluid. T-Microcantilever achieved 10.30  $\mu\text{m}$  overshoot point at time 0.215 sec, while others microcantilever

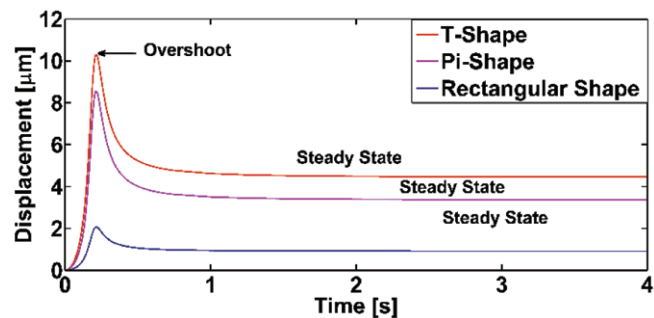


Figure 10 Displacement varies with time for T-microcantilever, Pi-microcantilever and rectangular microcantilever

are 8.55 Pa and 2.06 Pa respectively for Pi-microcantilever and rectangular microcantilever. The maximum points attained at a time of 0.235 seconds after that fluid becomes in steady state, there is no significant variation attained.

#### 4.7 Analysis fluid velocity of T-microcantilever at cut-off position

The coupling of fluid mechanics and structural mechanics module of software used to simulate fluid-structure interaction between fluid flow and flexible microcantilever structure in times domain study using laminar fluid flow. The fluid flow is 4.33 cm/sec across a microchannel, now the parabolic profile of fluid has different velocities at different cut-off points of the T-micro cantilever. The T-microcantilever placed at 200  $\mu\text{m}$  distance from the inlet position, analysis of fluid mechanics at four cutoff positions, position 1, position 2, position 3 and position 4. The cutoff point defines in 2D model is shown in above Fig.3 from the bottom to top surface of microcantilever. The T-microcantilever hinged structure, movable when fluid pressure applied on it, maximum velocity is 0.01482 m/sec attained at time 0.215 sec while the minimum velocity 0.00197 m/sec attained at 0.215 sec for position 4 and position 1 respectively. As seen Fig.11 graph between velocity and time, the velocity of fluid increased from cutoff point 1 to cut off point 4, its means at bottom of T-microcantilever fluid velocity is very low and when moved towards upper surface, the velocity is continually increased.

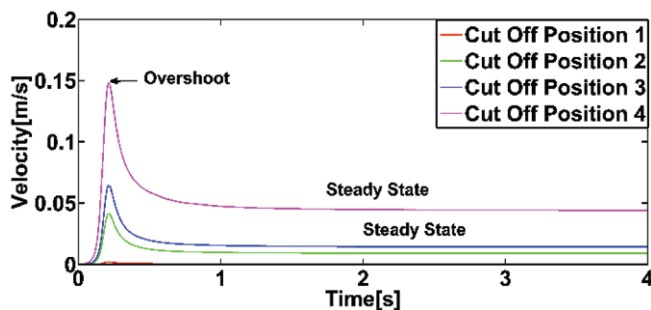


Figure 11: Velocity varies with time for T-microcantilever at cut off position

#### 4.8 Analysis fluid pressure of T-Microcantilever at cut-off position

This method measures pressure directly in microscale technique, the basic principle to measure a pressure of FSI by applying of fluid on T-microcantilever, four cut off point, and found at cut off point 1 overshoot value maximum attained 58.46 Pa while minimum value attained at cut off position 4. The Fig.12 shows pressure all four cut off position, and found after attained minimum value pressure became almost constant or steady state.

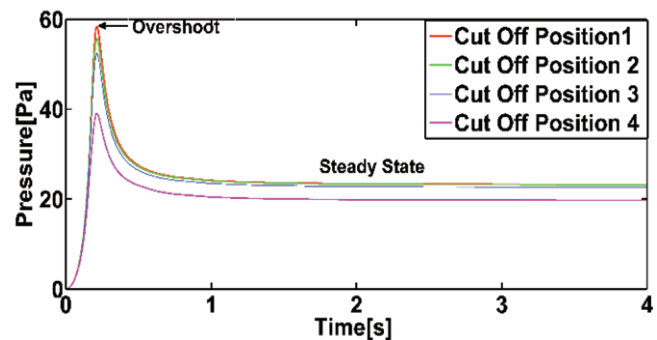


Figure 12: Pressure varies with time for T-microcantilever at cut off position

## 5.0 Conclusion

Simulated integrated microcantilever shows effective solutions for improving the pressure sensitivity and displacement of microcantilever by the utilizing concept of fluid structure interaction, which is responsible for enhancing maximum pressure with maximum deflection of microcantilever. Analysis of microfluidic pressure velocity, displacement, Reynold's number, and friction factor, microcantilever calculated, while almost same friction factor across a microchannel a, its concluded friction factor does not play an important role across a microchannel. The overshoot values at 0.215 seconds show maximum value in terms of velocity, pressure, and displacement. The cut-off points for fluidic analysis so that it gives high deflection in T- microcantilever. The integrated device is high pressure sensitive of fluid so that at minor or short duration got the highly precise value. The syringe set up size is very large, this method helps to reduce the size of such set up, and increased the efficiency, and reduces the cost of the device. The T-microcantilever gives the maximum displacement of 10.38  $\mu\text{m}$  at a time of 0.215 seconds. The simulation result shows behaviour of fluid when it interacts with solid. Integrated microcantilever with microchannel is pressure sensing mechanism is highly reliable, low cost and cost-effective technology which is highly suitable for biomedical microfluidics application such as pressure measurement in a syringe.

## 6.0 Acknowledgements

The authors would like to thank Multiscale Simulation Research Centre (MSRC), Manipal University Jaipur for providing simulation facilities of COMSOL Multiphysics 5.3.

## 7.0 References

1. Beebe, D. J., Mensing, G. A., & Walker, G. M. (2002): Physics and applications of microfluidics in biology. Annual review of biomedical engineering, 4(1), 261-286.

2. Shin, J. H., Lee, G. J., Kim, W., & Choi, S. (2016): A stand-alone pressure-driven 3D microfluidic chemical sensing analytic device. *Sensors and Actuators B: Chemical*, 230, 380-387.
3. Shields IV, C. W., Ohiri, K. A., Szott, L. M., & López, G. P. (2017): Translating microfluidics: Cell separation technologies and their barriers to commercialization. *Cytometry Part B: Clinical Cytometry*, 92(2), 115-125.
4. Dong, R., Liu, Y., Mou, L., Deng, J., & Jiang, X. (2019): Microfluidics based biomaterials and biodevices. *Advanced Materials*, 31(45), 1805033.
5. Saxena, A., Kumar, M., Gupta, A., Shrivastava, A., & Singh, K. (2021, August): Optimization of Microfluidic Pressure Sensing Mechanism Integrated Microcantilever in Microchannel. In 2021 International Conference on Recent Trends on Electronics, Information, Communication & Technology (RTEICT) (pp. 361-365). IEEE.
6. Lien, V., & Vollmer, F. (2007): Microfluidic flow rate detection based on integrated optical fiber cantilever. *Lab on a Chip*, 7(10), 1352-1356.
7. Quist, A., Chand, A., Ramachandran, S., Cohen, D., & Lal, R. (2006): Piezoresistive cantilever based nanoflow and viscosity sensor for microchannels. *Lab on a Chip*, 6(11), 1450-1454.
8. Pinto, R. M., Chu, V., & Conde, J. P. (2020): Label-free biosensing of DNA in microfluidics using amorphous silicon capacitive micro-cantilevers. *IEEE Sensors Journal*, 20(16), 9018-9028.
9. Noeth, N., Keller, S. S., & Boisen, A. (2014): Integrated cantilever-based flow sensors with tunable sensitivity for in-line monitoring of flow fluctuations in microfluidic systems. *Sensors*, 14(1), 229-244.
10. Basu, A. K., Basu, A., & Bhattacharya, S. (2020): Micro/nano fabricated cantilever based biosensor platform: A review and recent progress. *Enzyme and Microbial Technology*, 139, 109558.
11. Ricciardi, C., Canavese, G., Castagna, R., Ferrante, I., Ricci, A., Marasso, S. L., & Bussolino, F. (2010): Integration of microfluidic and cantilever technology for biosensing application in liquid environment. *Biosensors and Bioelectronics*, 26(4), 1565-1570.
12. Kuoni, A., Holzherr, R., Boillat, M., & de Rooij, N. F. (2003). Polyimide membrane with ZnO piezoelectric thin film pressure transducers as a differential pressure liquid flow sensor. *Journal of micromechanics and microengineering*, 13(4), S103.
13. Johansson, A., Calleja, M., Rasmussen, P. A., & Boisen, A. (2005): SU-8 cantilever sensor system with integrated readout. *Sensors and Actuators A: Physical*, 123, 111-115.
14. Raj, A., Suthanthiraraj, P., & Sen, A. K. (2018): Pressure-driven flow through PDMS-based flexible microchannels and their applications in microfluidics. *Microfluidics and Nanofluidics*, 22(11), 1-25.
15. Nezhad, A. S., Ghanbari, M., Agudelo, C. G., Packirisamy, M., Bhat, R. B., & Geitmann, A. (2012): PDMS microcantilever-based flow sensor integration for lab-on-a-chip. *IEEE Sensors journal*, 13(2), 601-609.
16. Kamat, A. M., Zheng, X., Jayawardhana, B., & Kottapalli, A. G. P. (2020): Bioinspired PDMS-graphene cantilever flow sensors using 3D printing and replica moulding. *Nanotechnology*, 32(9), 095501.
17. Shen, F., Ai, M., Ma, J., Li, Z., & Xue, S. (2020): An easy method for pressure measurement in microchannels using trapped air compression in a one-end-sealed capillary. *Micromachines*, 11(10), 914.
18. Johansson, A., Calleja, M., Rasmussen, P. A., & Boisen, A. (2005): SU-8 cantilever sensor system with integrated readout. *Sensors and Actuators A: Physical*, 123, 111-115.
19. Saxena, A., Kumar, M., & Singh, K. (2022): Analytical Study of Fluid Pressure-Sensing Mechanism in Microchannel for Microfluidic Device. In *Technology Innovation in Mechanical Engineering* (pp. 1045-1053). Springer, Singapore.
20. Noeth, N., Keller, S. S., & Boisen, A. (2014): Integrated cantilever-based flow sensors with tunable sensitivity for in-line monitoring of flow fluctuations in microfluidic systems. *Sensors*, 14(1), 229-244.
21. Bungartz, H. J., & Schäfer, M. (Eds.). (2006): Fluid-structure interaction: modelling, simulation, optimisation (Vol. 53). *Springer Science & Business Media*.
22. Rao, K. S., Sravani, K. G., Yugandhar, G., Rao, G. V., & Mani, V. N. (2015). Design and analysis of fluid structure interaction in a horizontal Micro Channel. *Procedia Materials Science*, 10, 768-788.
23. Saxena, A., & Agrawal, V. K. (2017): Comparative Study of Cantilever RF MEMS Switch. *Materials Today: Proceedings*, 4(9), 10328-10331
24. Tezduyar, T. E. (2003): Stabilized finite element methods for computation of flows with moving boundaries and interfaces. *Lecture Notes on Finite Element Simulation of Flow Problems (Basic-Advanced Course)*, *Japan Society of Computational Engineering and Sciences*, Tokyo, Japan.
25. Burger, J., Haldenwang, R., & Alderman, N. (2010): Friction factor-Reynolds number relationship for laminar flow of non-Newtonian fluids in open channels of different cross-sectional shapes. *Chemical Engineering Science*, 65(11), 3549-3556.
26. Singh, K., Akhtar, S., Varghese, S., & Akhtar, J. (2014): Design and development of MEMS pressure sensor characterization setup with low interfacing noise by using NI-PXI system. In *Physics of Semiconductor Devices* (pp. 449-451). Springer, Cham.